



**HAL**  
open science

## The Arabidopsis protein NPF6.2/NRT1.4 is a plasma membrane nitrate transporter and a target of protein kinase CIPK23

Laura Morales de los Ríos, Claire Corratgé-Faillie, Natalia Raddatz, Imelda Mendoza, Marika Lindahl, Alexis de Angeli, Benoit Lacombe, Francisco J Quintero, José M Pardo

### ► To cite this version:

Laura Morales de los Ríos, Claire Corratgé-Faillie, Natalia Raddatz, Imelda Mendoza, Marika Lindahl, et al.. The Arabidopsis protein NPF6.2/NRT1.4 is a plasma membrane nitrate transporter and a target of protein kinase CIPK23. *Plant Physiology and Biochemistry*, 2021, 168, pp.239-251. 10.1016/j.plaphy.2021.10.016 . hal-03713227

**HAL Id: hal-03713227**

**<https://hal.inrae.fr/hal-03713227>**

Submitted on 4 Jul 2022

**HAL** is a multi-disciplinary open access archive for the deposit and dissemination of scientific research documents, whether they are published or not. The documents may come from teaching and research institutions in France or abroad, or from public or private research centers.

L'archive ouverte pluridisciplinaire **HAL**, est destinée au dépôt et à la diffusion de documents scientifiques de niveau recherche, publiés ou non, émanant des établissements d'enseignement et de recherche français ou étrangers, des laboratoires publics ou privés.



Distributed under a Creative Commons Attribution - NonCommercial - NoDerivatives 4.0 International License



## The Arabidopsis protein NPF6.2/NRT1.4 is a plasma membrane nitrate transporter and a target of protein kinase CIPK23

Laura Morales de los Ríos<sup>a</sup>, Claire Corratgé-Faillie<sup>b</sup>, Natalia Raddatz<sup>a</sup>, Imelda Mendoza<sup>a</sup>, Marika Lindahl<sup>a</sup>, Alexis de Angeli<sup>b</sup>, Benoit Lacombe<sup>b</sup>, Francisco J. Quintero<sup>a, \*\*</sup>, José M. Pardo<sup>a, \*</sup>

<sup>a</sup> Institute of Plant Biochemistry and Photosynthesis (IBVF), Consejo Superior de Investigaciones Científicas and Universidad de Sevilla, 41092, Seville, Spain

<sup>b</sup> Biochimie et Physiologie Moléculaire des Plantes, Univ. Montpellier, CNRS, INRAE, 34060, Montpellier Cedex, France

### ARTICLE INFO

#### Keywords:

Plant nutrition  
Nitrate  
Potassium  
Ion transport  
Arabidopsis

### ABSTRACT

Nitrate and potassium nutrition is tightly coordinated in vascular plants. Physiological and molecular genetics studies have demonstrated that several NPF/NRT1 nitrate transporters have a significant impact on both uptake and the root-shoot partition of these nutrients. However, how these traits are biochemically connected remain controversial since some NPF proteins, e.g. NPF7.3/NRT1.5, have been suggested to mediate  $K^+/H^+$  exchange instead of nitrate fluxes. Here we show that NPF6.2/NRT1.4, a protein that gates nitrate accumulation at the leaf petiole of *Arabidopsis thaliana*, also affects the root/shoot distribution of potassium. We demonstrate that NPF6.2/NRT1.4 is a plasma membrane nitrate transporter phosphorylated at threonine-98 by the CIPK23 protein kinase that is a regulatory hub for nitrogen and potassium nutrition. Heterologous expression of NPF6.2/NRT1.4 and NPF7.3/NRT1.5 in yeast mutants with altered potassium uptake and efflux systems showed no evidence of nitrate-dependent potassium transport by these proteins.

### 1. Introduction

Nitrate ( $NO_3^-$ ) is the main nitrogen source for most land plants and constitutes a major fertilizer input in agriculture. Significant progress has been made in understanding the multilayered transport processes enabling nitrate acquisition from the soil and distribution into different plant organs and tissues. We are also learning how nitrate availability is perceived and signaled, and how the nitrogen status is communicated between shoots and roots (Wang et al., 2018, 2021).

Nitrate transporters are critical for both nutrition and signaling (Wang et al., 2018). Four protein families are involved in nitrate transport, the NITRATE TRANSPORTER 1 (NRT1)/PEPTIDE TRANSPORTER (PTR) family (NPF), NITRATE TRANSPORTER 2 (NRT2), CHLORIDE CHANNEL (CLC), and SLOWLY-ACTIVATING ANION CHANNEL and their homologs (SLAC/SLAH). The coordinated activity of these proteins governs nitrate uptake, translocation, and storage in vacuoles. The panoply of nitrate transporters enables plants to adapt to a

wide range of nitrate concentrations in the soil and in different plant tissues. Accordingly, plants display nitrate uptake by Low-Affinity (LATS) and High-Affinity (HATS) Transport Systems, which broadly correspond to the activity of NPF/NRT1 and NRT2 transporters, respectively.

There are 53 and 93 *NPF* genes in *Arabidopsis* and rice, respectively (Leran et al., 2014). The Arabidopsis NPF protein family has been subdivided into 8 clades based on sequence phylogeny and, as detailed characterization of individual members is showing, a diverse range of substrates (Corratgé-Faillie and Lacombe, 2017). Most NPF transporters display capacity for nitrate transport with low affinities and operate in LATS. Exceptions are the Arabidopsis CHL1/NPF6.3/NRT1.1 and rice OsNRT1.1B/OsNPF6.5 that display dual affinities, being able to toggle between high (micromolar) and low (millimolar) affinities in a process that requires phosphorylation by the CBL-INTERACTING PROTEIN KINASE 23 (CIPK23) (Wang et al., 2018, 2020). The *Arabidopsis* genome encodes 7 NRT2 proteins, which generally behave as high-affinity

\* Corresponding author. Institute of Plant Biochemistry and Photosynthesis (IBVF), Consejo Superior de Investigaciones Científicas and Universidad de Sevilla, cicCartuja, 41092, Seville, Spain.

\*\* Corresponding author. Institute of Plant Biochemistry and Photosynthesis (IBVF), Consejo Superior de Investigaciones Científicas and Universidad de Sevilla, cicCartuja, 41092, Seville, Spain.

E-mail address: [jose.pardo@csic.es](mailto:jose.pardo@csic.es) (J.M. Pardo).

<https://doi.org/10.1016/j.plaphy.2021.10.016>

Received 31 August 2021; Received in revised form 7 October 2021; Accepted 9 October 2021

Available online 11 October 2021

0981-9428/© 2021 Consejo Superior de Investigaciones Científicas. Published by Elsevier Masson SAS. This is an open access article under the CC BY-NC-ND

license (<http://creativecommons.org/licenses/by-nc-nd/4.0/>).

nitrate transporters (HATS). With sufficient nitrate supply, the dual-affinity transporter NPF6.3/NRT1.1 and the low-affinity transporter NPF4.6/NRT1.2 account for most the root nitrate uptake in *Arabidopsis* (Noguero and Lacombe, 2016). Under nitrate-limiting conditions, the NRT2 family plays a predominant role in nitrate acquisition from the soil.

Transporters of both families NPF and NRT2 belong to the Major Facilitator Superfamily (MFS) of secondary active transporters and are dependent on protons for nitrate transport. Notably, members of the NPF family display a surprisingly broad substrate specificity, including nitrate, nitrite, chloride, dipeptides and hormones (auxin, abscisic acid, gibberellins, glucosinolates and jasmonoyl-isoleucine) (Wang et al., 2018). Some of these transporters are even capable of accepting more than one substrate (e.g. nitrate/auxin, nitrate/ABA, nitrate/glucosinolates, or GA/JA) (Corratgé-Faillie and Lacombe, 2017). How the NRT1/PTR family has evolved to recognize such diverse substrates is a matter of speculation. The crystal structure of NF6.3/NRT1.1 indicates that only minor changes in the evolutionarily related peptide-binding site of PTR transporters are required to accommodate nitrate in the NF6.3/NRT1.1 protein. These changes are predominantly located in the C-terminal bundle of the MSF fold, whereas the proton coupling determinants that have remained conserved reside largely in the N-terminal bundle. Thus, the ability of the NRT1/PTR family to recognize multiple ligands may stem from the physical separation of these two domains, giving greater freedom to the C-terminal bundle to evolve to recognize different nitrogenous ligands (Parker and Newstead, 2014).

Another intriguing phenomenon is that the activity of some NPF proteins impinges greatly in potassium ( $K^+$ ) nutrition and its root-shoot partition (Li et al., 2017; Fang et al., 2020; Raddatz et al., 2020). The classical view to explain the tight connections between these nutrients is that nitrate and  $K^+$  function as reciprocal counterions in transport processes thereby affecting each other, especially in the long-distance transport along the vascular system (Raddatz et al., 2020). However, two members of the NPF7 clade, NPF7.3/NRT1.5 and NPF7.2/NRT1.8, have been described to directly transport  $K^+$  in exchange for  $H^+$ , despite the fact that these proteins had been characterized previously as *bona fide* nitrate transporters. The *Arabidopsis* NPF7.3/NRT1.5 protein was first described as a nitrate-efflux transporter located in xylem-pole pericycle cells (Lin et al., 2008). In *nrt1.5* KO mutants, lesser nitrate was detected in the xylem sap transported to shoots, indicating that NPF7.3/NRT1.5 mediates xylem loading of nitrate in roots (Lin et al., 2008). NPF7.2/NRT1.8 is expressed in xylem parenchyma cells, and more nitrate was found in the xylem sap of the *nrt1.8* KO mutant compared to the wild-type (Li et al., 2010). The antagonistic nitrate fluxes determined by NPF7.3/NRT1.5 and NPF7.2/NRT1.8 are also reflected in their  $K^+$  profiles (Lin et al., 2008; Drechsler et al., 2015; Meng et al., 2016; Zheng et al., 2016; Li et al., 2017). Recently, a mutant allele of NRT1.5 was recovered as the LOW-POTASSIUM SENSITIVE *lks2* locus of *Arabidopsis* (Li et al., 2017). Evidence was also presented supporting that NPF7.3/NRT1.5/LKS2 functions as a proton-coupled  $K^+/H^+$  antiporter that mediates  $K^+$  release out of root parenchyma cells and facilitate  $K^+$  loading into the xylem (Li et al., 2017). However, the nitrate transporter and sensor NPF6.3/NRT1.1 is also required for plant growth under  $K^+$ -limiting conditions since the *nrt1.1* mutant shows disturbed  $K^+$ -uptake and root-to-shoot allocation (Fang et al., 2020). Detailed analyses indicated that these  $K^+$ -related interactions were dependent on  $H^+$ -consumption associated with the  $H^+/NO_3^-$  symport mediated by NRT1.1, which in turn affected the operation of  $K^+$  channels and transporters relevant to  $K^+$  uptake and root-to-shoot partition under  $K^+$ -limiting conditions (Fang et al., 2020). Therefore, whether some NPF/NRT1 proteins are able to transport  $K^+$  remains controversial (Raddatz et al., 2020).

Our ongoing research on  $K^+$  nutrition indicates that the *Arabidopsis* NPF6.2/NRT1.4 protein affects  $K^+$  uptake and root-shoot partitioning. NPF6.2/NRT1.4 is preferentially expressed in the leaf petiole and midrib. Compared to the wild-type, a *nrt1.4* KO mutant showed reduced

nitrate content in the petiole and increased content in the leaf blade, suggesting that NPF6.2/NRT1.4 gates negatively the passage of nitrate to the leaf (Chiu et al., 2004). Electrophysiological characterization in *Xenopus* oocytes indicated that NPF6.2/NRT1.4 transports nitrate with low-affinity, but no dipeptides, as expected from members of NPF-clade 6 (Chiu et al., 2004; Wang et al., 2018). However, the subcellular localization of NRT1.4 was not determined, and the gating of nitrate by NPF6.2/NRT1.4 could result from nitrate influx or intracellular accumulation at the petiole. To clarify the precise subcellular localization of NPF6.2/NRT1.4 and to explore whether this protein could also use  $K^+$  as substrate, as it has been described for NPF7.3/NRT1.5 and NPF7.2/NRT1.8, we have expressed NPF6.2/NRT1.4 in *Nicotiana benthamiana*, the nitrate-assimilating yeast *Hansenula polymorpha* and in strains of *Saccharomyces cerevisiae* defective in transporters governing  $K^+$  uptake and efflux. Our results indicate that NPF6.2/NRT1.4 is a plasma membrane nitrate-transporter that gives no indication of being able to transport  $K^+$  with and without accompanying nitrate. Similar results were obtained for NPF7.3/NRT1.5. We also show that NPF6.2/NRT1.4 is a target of the CIPK23 kinase that coordinately controls nitrogen use (nitrate and ammonium) and  $K^+$  nutrition (Raddatz et al., 2020).

## 2. Materials and methods

### 2.1. Isolation of homozygous *nrt1.4* T-DNA insertion mutant

Seeds from the *nrt1.4* line WiscDsLox322H05, Col-0 ecotype, were obtained from the Nottingham Arabidopsis Stock Centre (NASC; Nottingham University, UK). This mutation corresponds to allele *nrt1.4-2* described earlier (Chiu et al., 2004). Plants of genotype *nrt1.4*, homozygous for the T-DNA insertion, were identified by genotyping the segregating population. Plants of the Col-0 ecotype were used as wild-type NRT1.4 control. Primers used for the diagnostic PCR were P745 (5'-AACGTCGCAATGTGTTATTAAGTTGTC-3') annealing to the T-DNA left border, NRT1.4-forward (5'-GATGAACCTATCTCAAAGATTT CACGTTT-3') and NRT1.4-reverse (5'-AGAAGAGTCCAGTGCTCATAGT TTTCATT-3'). Amplicons for wild-type NRT1.4 and mutant *nrt1.4* alleles were 3.5 kb (NRT1.4-forward and NRT1.4-reverse primers) and 2.7 kb (P745 and NRT1.4-reverse primers), respectively.

### 2.2. *Arabidopsis* growth conditions and nutrient content

Seeds of *Arabidopsis thaliana* ecotype Col-0 and the *nrt1.4-2* knock-out mutant were stratified for 3d at 4 °C, and then germinated at room temperature in plastic holders containing mineral wool imbibed with distilled water. Seedlings were transferred to plastic containers for hydroponic culture in LAK medium (Barragan et al., 2012) containing 1 mM  $K^+$ ; nitrate at either 0.5 mM or 4 mM was added as  $Ca(NO_3)_2$ . Hydroponic pots were incubated for 5 weeks in a controlled growth chamber with the day/night regime of 20/18 °C, 70% relative humidity, 8/16 h light/darkness cycle, and 120–140  $\mu\text{mol m}^{-2} \text{s}^{-1}$  PAR. For determination of nutrient content, 5-week old plants were separated into shoots and roots. Dry weight was measured after drying samples at 65 °C for 72 h in a forced-air oven. Potassium and nitrate were extracted by heating ground material in water at 75 °C for 2 h. Potassium was measured by ICP-OES, and nitrate content was determined by colorimetric assay with a microplate spectrophotometer (Cataldo et al., 1975).

Nitrate content in petioles and leaf lamina was measured following Chiu et al. (2004) with modifications. The third rosette leaves from three individual plants were excised from Col-0 and the *nrt1.4-2* mutant, which were grown for 3 weeks in soil in an environmentally controlled growth chamber (70% relative humidity, day/night regime of 20/18 °C and 16/8 h illumination, with 120–140  $\mu\text{mol m}^{-2} \text{s}^{-1}$  PAR). Detached leaves were dissected into petioles and lamina, then 100  $\mu\text{l}$  of milli-Q water was added, the mixture boiled for 20 min and frozen at –20 °C overnight. The material was centrifuged at 20,800 g for 5 min at RT and

the nitrate content was determined in the supernatant. Soluble proteins were measured by Bradford method (Bio-Rad Protein Assay), and used as reference for normalization of the nitrate content.

### 2.3. Isolation and cloning of the *NRT1.4* cDNA from *Arabidopsis thaliana*

The full-length cDNA of *NRT1.4* (At2g26690) was amplified by PCR from total cDNA of *Arabidopsis thaliana* Col-0 ecotype using the forward primer 5'-ATGGAGAGCAAAGGGAGTTGGA-3' and reverse primer 5'-TCAGCAGTCTTCAACTGAAAATC-3' (start and stop codons are underlined) and the amplified product was cloned into pSpark® (Canvax Biotech) producing the construct pSpark®-*NRT1.4*. The *NRT1.4* cDNA was verified by sequencing.

### 2.4. Yeast methods

The transport activity of *NRT1.4* was tested in the yeasts *Hansenula polymorpha* and *Saccharomyces cerevisiae*.

For expression in *Hansenula polymorpha*, the *NRT1.4* ORF was amplified by PCR using pSpark®-*NRT1.4* as template and the forward primer 5'-ATCAGGGTGCACATGGAGAGCAAAGGGAGTTGG-3' and reverse primer 5'-GCCGCACTAGTGGATCCTGATTCAGC-3', which contained *SalI* and *SpeI* sites (underlined). The PCR product was digested with *SalI* and *SpeI* restriction enzymes and cloned in the integrative pYNR-EX vector cut with the same enzymes (Martin et al., 2008). The resulting plasmid was linearized using a *BstEII* site located in the *LEU2* marker before transformation. *H. polymorpha* strains used in this work are derivatives of NCYC495 (*leu2 ura3*) (Sudbery et al., 1988). The mutant strain  $\Delta ynt1$  created by insertional mutagenesis with *URA3* ( $\Delta ynt1::URA3$ ) and the prototrophic control strain (*leu2::p18B1(LEU2) ura3::pBSURA3 (URA3)*) have been described elsewhere (Pérez et al., 1997). Strain  $\Delta ynt1$  was used for genetic complementation with *NRT1.4*. Plasmids were transformed by electroporation (Sudbery et al., 1988). Single yeast colonies were grown 16h at 37 °C and shaking in YGNH medium (Yeast Nitrogen Base 0.17% (w/v), 2% glucose, 5 mM NH<sub>4</sub>Cl as nitrogen source) (Martin et al., 2008). For cell growth experiments, centesimal and millesimal dilutions of cell cultures at DO<sub>660</sub> ~ 1 were incubated in the same medium without nitrogen source (YG) plus 0,5 mM KNO<sub>3</sub> for 48 h. Yeast growth was measured in a microplate-reader Varioskan™ LUX (Thermo Scientific) and expressed as DO<sub>660</sub>.

For expression in *S. cerevisiae*, the complete *NRT1.4* coding region without stop codon was amplified from pSpark®-*NRT1.4* by PCR using the forward primer 5'-ATGGAGAGCAAAGGGAGTTGGA-3' and the reverse primer 5'-GTGGATCCTCGAGAGCAGTCTCAAC-3'. The amplicon was cloned between *SmaI* and *XhoI* in the pYPGE15 expression vector (Brunelli and Pall, 1993) that had been previously modified introducing the GFP coding sequence between the *KpnI* and *XhoI* restriction sites. GFP images were acquired by epifluorescence microscopy with a Zeiss AxioScope equipped with a filter set Chroma 41018 (exciter HQ470/40, emitter HQ500LP). The cDNAs of *CIPK23* and *CBL1* were expressed together using the yeast expression vector p414GPD (Ródenas et al., 2021). The yeast expression vector p416GPD containing the *NRT1.5* cDNA has been described elsewhere (Li et al., 2017). *AKT1* from pFL61-*AKT1* (Sentenac et al., 1992) was cloned in vector PRS415 using *XbaI* and *BamHI* restriction sites.

The *S. cerevisiae* strains TTE9.3 (MAT $\alpha$ , *ena1Δ::HIS3::ena4Δ*, *leu2*, *ura3-1*, *trp1-1*, *ade2-1*, *trk1Δ*, *trk2::pCK64*) (Bañuelos et al., 1995), AXT3K (MAT $\alpha$ , *ena1Δ::HIS3::ena4Δ*, *nha1::LEU2*, *nhx1::KanMX ura3-1 trp1 ade2-1 Kan1-100*) (Quintero et al., 2002) and W303-1A (MAT $\alpha$  *ura3-1 leu2-3,112 his3-11,15 trp1-1 ade2-1 kan1-100*) (Wallis et al., 1989) were used for genetic complementation with *NRT1.4*, *NRT1.5* and *CIPK23/CBL1*. Plasmids were transformed into the yeast strains using the PEG-lithium acetate protocol (Gietz and Schiestl, 2007). For growth complementation assays, 5  $\mu$ l aliquots from saturated yeast cultures (DO<sub>660</sub> = 1) or 10-fold serial dilutions were spotted onto different media: AP plates (Rodríguez-Navarro and Ramos, 1984) supplemented

with KCl or KNO<sub>3</sub> at the concentrations indicated in each experiment; or YPD pH 5.5 plates (1% yeast extract, 2% peptone and 2% glucose) supplemented with 1.5 M KCl. Resistance to hygromycin B was assayed in YPD medium. Plates were incubated at 28 °C for 3–4 days.

### 2.5. In-vitro phosphorylation assays

A fragment of 33 bp of the *NRT1.4* cDNA encoding a peptide from amino acids Phe92 to Phe102 was amplified by PCR with the forward primer 5'-CGCGGATCCTTCTCGGGTCTTTCAAACCATCGGTATCTTCTGACTGACGATCTGCTCGCGGTTTCG-3' containing a *BamHI* site and the reverse primer 5'-GTTGCCATTGTCGAGGCATCG-3' with a *PstI* site. The amplicon was cloned between *BamHI* and *PstI* restriction sites of the pGEX4T1 vector to generate pGEX4T1-*NRT1.4*. The T98A mutation was generated by PCR with primers 5'-CGCGGATCCTTCTCGGGTCTTTCAAAGCAATCGGTATCTTCTGACTGACGATCTGCTCGCGGTTTCG-3' and 5'-GTTGCCATTGTCGAGGCATCG-3' to produce pGEX4T1-*NRT1.4*-T98A. The Velocity polymerase (Bioline) was used for all the PCR amplifications. The PCR products were verified by sequencing.

Glutathione-S-transferase (GST) fusion proteins with *NRT1.4* fragments were expressed in Rosetta 2 (DE3) pLysS cells (Stratagene) by induction at 0.7 OD<sub>600</sub> with 0.5 mM isopropyl- $\beta$ -D-thiogalactoside (IPTG) for 16 h at 30 °C and shaking. Bacterial cells were collected by centrifugation and the pellets were resuspended in a solution containing 20 mM Tris-HCl pH 7.8, 150 mM NaCl, 10 mM DTT. Cells were lysed by sonication and the fusion proteins were purified by affinity-chromatography using Glutathione Sepharose 4B (GE Healthcare) (Harper and Speicher, 2008). GST-*NRT1.4* and GST-*NRT1.4*-T98A proteins were concentrated to ~0.5 mg ml<sup>-1</sup>. The sample purity was determined by SDS-PAGE.

Casein protein (Duchefa), GST-*NRT1.4* and GST-*NRT1.4*-T98A, 2  $\mu$ g each, were subjected to phosphorylation by the CIPK23- $\Delta$ C-T190D protein kinase (Chaves-Sanjuan et al., 2014) in 20  $\mu$ l of buffer (20 mM Tris-HCl pH 7.5; 5 mM MgCl<sub>2</sub>, 1 mM DTT). Reactions were started by adding ATP (0.5 mM with 20  $\mu$ Ci of [ $\gamma$ -<sup>32</sup>P] ATP), incubated at 30 °C for 30 min, and then stopped with 5.5  $\mu$ l of 5x SDS/PAGE sample buffer. Proteins were separated by SDS/PAGE using a 12% (w/v) acrylamide gel. Radioactivity was detected on the dry gels by autoradiography in a Cyclone® Plus Storage Phosphor System (PerkinElmer).

### 2.6. Agrobacterium-mediated transient expression in *Nicotiana benthamiana*

For transient expression in *Nicotiana benthamiana*, the cDNA of *NRT1.4* without the stop codon was first cloned in pDONR™201 vector (Invitrogen Life Technologies) and then transferred to plasmid pGWB605 (Nakamura et al., 2010) in-frame to GFP through an LR recombination reaction using Gateway® LR Clonase™ II Enzyme Mix (Invitrogen). The vector encoding the *A. thaliana* CBL1 protein fused to OFP was obtained from J. Kudla's lab (Ma et al., 2019) and was used as plasma membrane marker. *NRT1.4*-GFP and CBL1-OFP fusions were expressed under the control of the *CaMV35S* promoter. *N. benthamiana* agroinfiltration was performed according to (Waadt et al., 2008). Tobacco plants were grown in a greenhouse at 25/20  $\pm$  2 °C with a 16-h light/8-h dark regime. *NRT1.4*-GFP and CBL1-OFP were mobilized into *Agrobacterium tumefaciens* strain GV3101 by electroporation followed by selection on LB plates containing the appropriate antibiotics. For transient expression, *Agrobacterium* transformants containing the plasmid constructs and the p19 silencing suppressor plasmid were grown at an OD<sub>600</sub> of 0.5, 0.5 and 0.6, respectively, and co-infiltrated in 5-week-old *N. benthamiana* leaves. Forty-eight hours after inoculation, *Agrobacterium*-infected cells of the lower epidermis of leaves were analyzed with a Confocal Laser Scanning Microscope FLUOVIEW FV3000 (Olympus). To image GFP fluorescence, the 488 nm laser line was used for excitation, and emission was collected between 510 and 550 nm. For imaging OFP, excitation was at 561 nm and emission was captured

between 570 and 620 nm. Fluorescence of both channels was captured simultaneously. Further imaging analyses were done with the Fiji software.

### 2.7. $^{15}\text{N}$ -nitrate accumulation assay in *Xenopus* oocytes

For expression in *Xenopus* oocytes, the pSpark-NRT1.4 plasmid was digested with *Stu*I and *Bam*HI and the DNA fragment containing *NRT1.4* was cloned into vector pNB1u (Nour-Eldin et al., 2006) between the *Sma*I and *Bgl*II sites. Constructs pGEMKN-CIPK23 and pGEMKN-CBL1 have been described elsewhere (Geiger et al., 2009; Held et al., 2011). Plasmids pNB1u-NRT1.4, pGEMKN-CIPK23 and pGEMKN-CBL1 were linearized, and transcribed *in vitro* with HiScribe T7 ARCA mRNA Kit (New England Biolabs), following the manufacturer's protocol. Oocytes were obtained and injected as previously described (Lacombe and Thi-baud, 1998). Two days after injection with different combinations of mRNA, injected and control (water-injected) oocytes were incubated 2 h in 2 mL of ND96 medium (2 mM KCl, 96 mM NaCl, 1 mM MgCl<sub>2</sub>, 1.8 mM CaCl<sub>2</sub>, 5 mM MES/Tris, pH 5.5) containing 30 mM of K<sup>15</sup>NO<sub>3</sub> (atom % <sup>15</sup>N abundance: 99.9%, Sigma-Aldrich) to test influx activity (Léran et al., 2015). Oocytes were then washed 5 times in 15 mL of ND96 medium (pH 5.5) at 4 °C and dried at 65 °C during 24 h. Oocytes were then analyzed for <sup>15</sup>N abundance by Continuous Flow Mass Spectrometry, using an Euro-EA Eurovector elemental analyzer (VarioPyroCUBE, Elementar, UK) coupled with an IsoPrime Precision mass spectrometer (Elementar, UK).

## 3. Results

### 3.1. *NPF6.2/NRT1.4* is a plasma membrane nitrate transporter

The *Arabidopsis* protein NRT1.4 (gene *At2g26690*) has been reported to function as a low-affinity nitrate transporter in *Xenopus* oocytes (Chiu et al., 2004), but the precise subcellular localization of NRT1.4 in plants has not been determined. Hence, a translational fusion NRT1.4-GFP was co-expressed in *Nicotiana* leaves together with a plasma membrane marker comprising the *Arabidopsis* CBL1 protein C-terminally tagged with OFP. The Calcineurin B-like 1 protein (CBL1) is recruited to the plasma membrane owing to its co-translational N-myristoylation of residue Gly-2 and subsequent palmitoylation at Cys-3 (Batistic et al., 2008). Analysis of fluorescence intensity in the green (GFP) and red (OFP) channels captured simultaneously in a laser scanning microscope showed that both proteins NRT1.4-GFP and CBL1-OFP co-localized in transects across the plasma membrane (Fig. 1), thus supporting a role for NRT1.4 in nitrate uptake.

Next, we produced homozygous loss-of-function *nrt1.4* mutant plants. For this, we obtained from the public repository at NASC the line *WiscDsLox322H05* bearing a T-DNA insertion in the second intron of *NRT1.4* (*At2g26690*). This mutant allele corresponds to the knock-out line *nrt1.4-2* described by Chiu et al. (2004). Wild-type Col-0 and *nrt1.4-2* plants were grown in hydroponic culture in LAK medium formulated to contain 4 mM NO<sub>3</sub><sup>-</sup> and 1 mM K<sup>+</sup>. Analysis of the nitrate content of in leaf petiole and lamina of *nrt1.4-2* and wild-type plants confirmed that the petiole of mutant plants had a much lower nitrate content than control plants (Fig. 2a). However, in our experimental

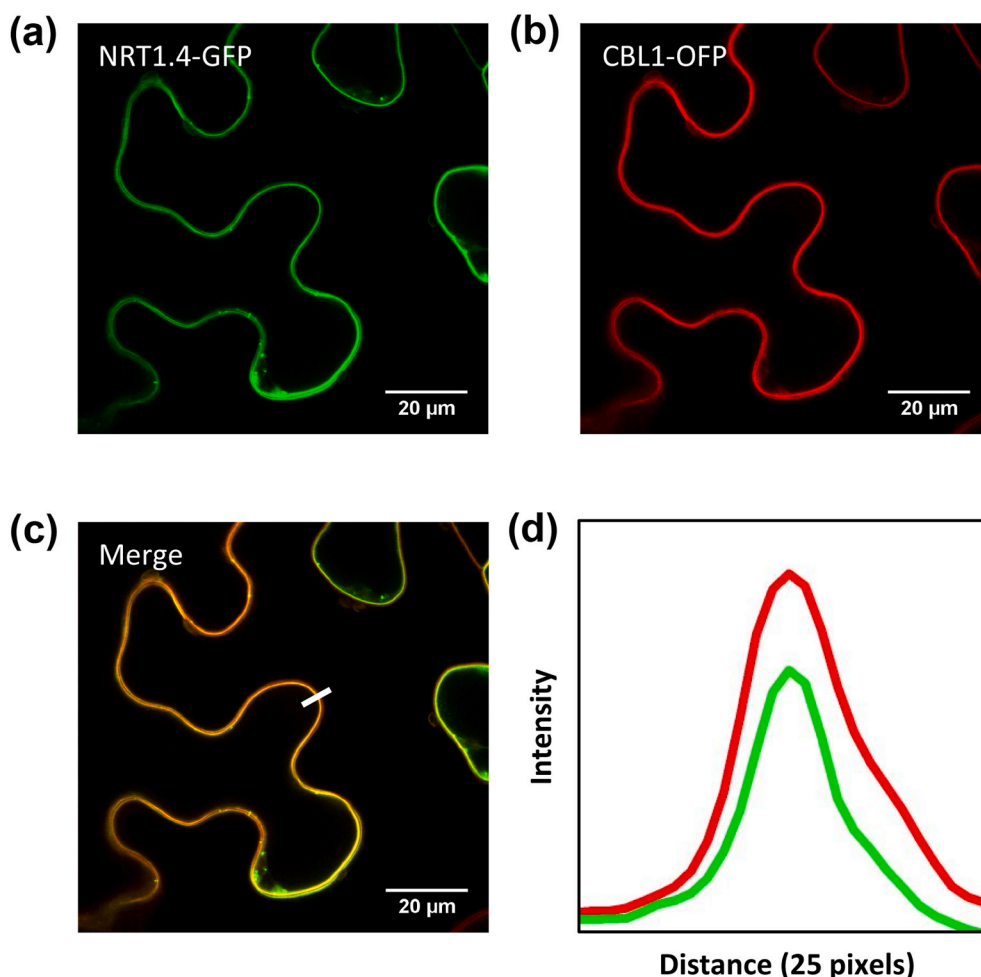


**Fig. 1.** Subcellular localization of NRT1.4-GFP (a) and CBL1-OFP (b) in *Nicotiana benthamiana* epidermal cells. The fluorescence of GFP and OFP was monitored 2-day post-agroinfiltration using confocal laser scanning microscopy. (c) NRT1.4 and CBL1 co-localize in the plasma membrane. (d) The fluorescence intensity profile of GFP (green) and OFP (red) proteins in a transect across the cell surface (length = 25 pixels). (For interpretation of the references to color in this figure legend, the reader is referred to the Web version of this article.)

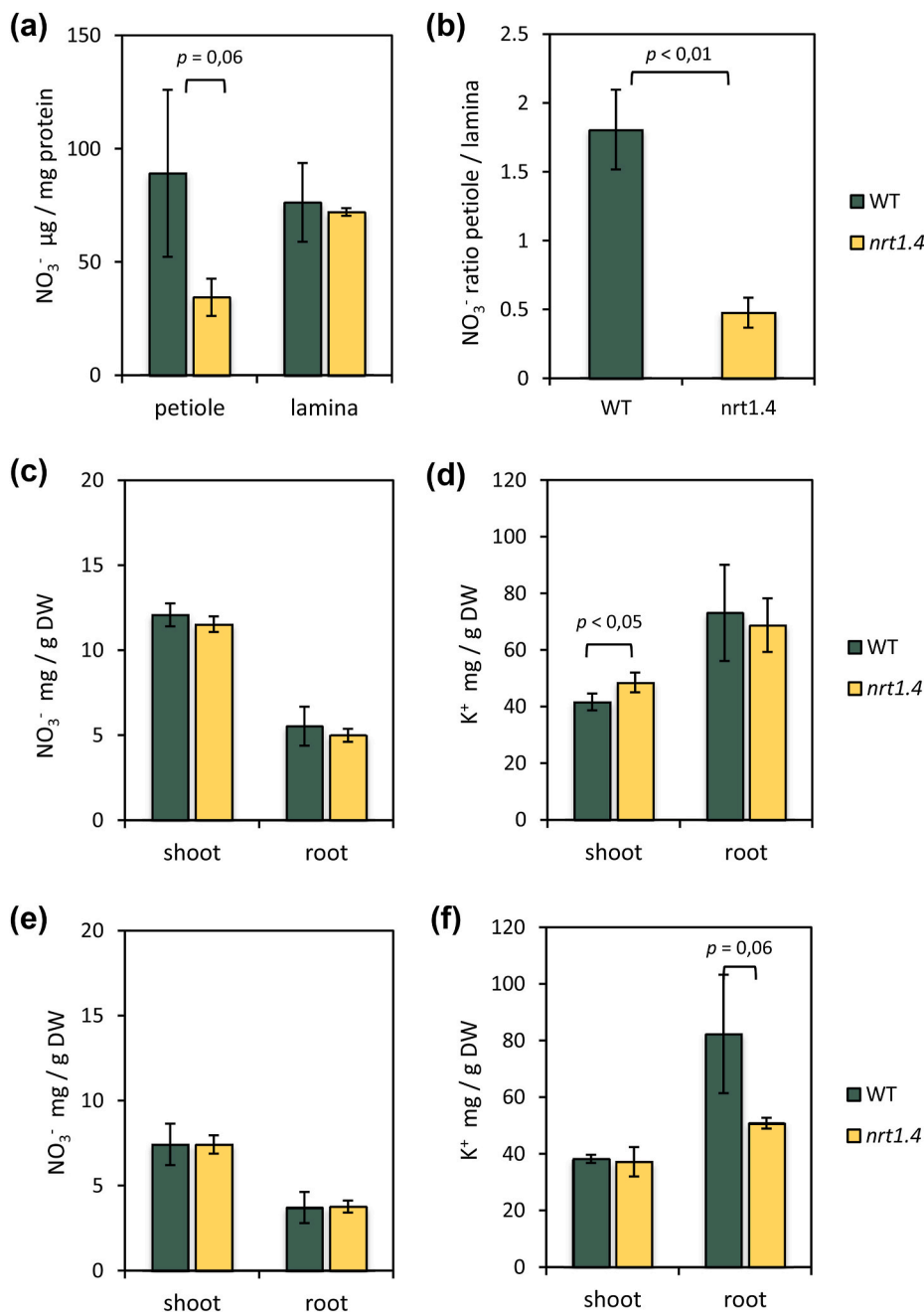


**Fig. 2.** Nitrate and potassium contents in the *knock-out* mutant *nrt1.4*. (a,b) Petioles and leaf lamina of 3-week old plants grown in soil were separated and had their nitrate and soluble protein contents determined. Bars are mean and SD ( $n = 3$ ) (c,d) Plants were grown in hydroponic culture with LAK solution containing 1 mM  $\text{K}^+$  and 4 mM  $\text{NO}_3^-$  for 5 weeks. Shoots and roots were separated for determination of nitrate and potassium contents. Values are expressed as mg of nutrient per gram of dry-weight. Bars are mean and SD ( $n = 6$ ). (e,f) Nitrate and potassium contents in the shoot and roots of plants grown in LAK solution containing 1 mM  $\text{K}^+$  and 0,5 mM  $\text{NO}_3^-$  ( $n = 3$ ). Statistical significance was determined with a *t*-test and *p* values of significant differences are indicated above brackets.

conditions, we did not detect a significant difference in the nitrate content in the lamina. Nevertheless, these data corroborate that mutation *nrt1.4-2* produces an statistically significant difference in the nitrate content ratio between the petiole and lamina compared to the wild-type (Fig. 2b), thus supporting a role for NRT1.4 in gating nitrate flux at the leaf petiole (Chiu et al., 2004).

We next determined  $\text{NO}_3^-$  and  $\text{K}^+$  contents in shoots and roots of *nrt1.4* plants grown in 4 mM  $\text{NO}_3^-$  and 1 mM  $\text{K}^+$ . Analyses of the plant mineral content showed that *nrt1.4-2* had a disturbed  $\text{K}^+$  partition between roots and shoots compared to the wild-type control (Fig. 2d). The higher  $\text{K}^+$  content in the shoots of *nrt1.4-2* plants was statistically significant ( $p < 0.05$ , *t*-test). This resulted in a 1.42 root/shoot ratio of  $\text{K}^+$  content in the mutant compared to the 1.75 ratio value in the wild-type. Again, no significant differences were found in the nitrate contents or the root/shoot ratio between control and *nrt1.4-2* plants in our experimental conditions (Fig. 2c).

To test whether limited nitrate availability modified further the shoot/root distribution of  $\text{K}^+$ , plants were grown in 0,5 mM  $\text{NO}_3^-$  and 1 mM  $\text{K}^+$  and had their mineral contents determined. In these conditions, the difference in the  $\text{K}^+$  content in shoots of wild-type and *nrt1.4* plants was cancelled and instead they showed differences in the root  $\text{K}^+$  content, being it lower in the mutant ( $p = 0,059$ , *t*-test). The comparison of the average  $\text{K}^+$  contents at different nitrate availabilities (Fig. 2d, f) indicated that low-nitrate specifically reduced the  $\text{K}^+$  content in the root of the *nrt1.4* mutant, with little effect on the wild-type that maintained similar root  $\text{K}^+$  contents in the two nitrate conditions. As expected, reducing the nitrate supplement from 4 mM to 0.5 mM brought about the corresponding decrement in the nitrate contents in plant tissues (Fig. 2c, e), but no differences between wild-type and *nrt1.4* mutant plants were found.

Next, we tested whether NRT1.4 mediated nitrate uptake in *H. polymorpha*. This soil yeast is unique in its capacity to take up and

assimilate nitrate into organic matter (Siverio, 2002). Genes *YNT1*, *YNR1* and *YNI1* encode proteins with nitrate transporter, nitrate reductase and nitrite reductase activities, respectively. Protein *YNT1* is the only nitrate uptake system in *Hansenula*, which makes the *ynt1* loss-of-function mutant a suitable tool for evaluating the nitrate transport capacity of heterologous transport proteins (Martin et al., 2008). The full-length cDNA of *NRT1.4* was cloned into the integrative vector pYNR-EX under the control of the nitrogen-inducible *YNR1* gene promoter (Martin et al., 2008). The resulting plasmid was linearized at the *LEU2* marker before transformation of the  $\Delta ynt1$  mutant strain. Twenty independent transformants were screened for growth in YG plates (no nitrogen source) with and without supplemental 0.5 mM  $KNO_3$ . Next, the growth rate of 10 individual clones able to grow only in the nitrate-containing medium was measured using the  $\Delta ynt1$  strain transformed with empty vector and the wild-type *YNT1* strain as controls. The results showed that *NRT1.4* supported the nitrate-dependent growth of  $\Delta ynt1$  cells at ca. half the rate of the *YNT1* control strain and well above the 16% background growth achieved by the  $\Delta ynt1$  transformants with empty vectors (Fig. 3). This result, together with the plasma membrane localization, confirms that *NRT1.4* is indeed a nitrate uptake protein.

### 3.2. CIPK23 phosphorylates *NRT1.4*

The growth of *NRT1.4*-expressing *Hansenula* cells in YG medium with nitrate as the sole nitrogen source was not as robust as that of the *YNT1* control, despite the use of the *YNR1* promoter for *NRT1.4* expression (Fig. 3). *NPF6.2/NRT1.4* is the closest homolog of the transporter and nitrate-sensor protein *NPF6.3/NRT1.1* in the NPF family of *Arabidopsis* (Fig. 4) (Leran et al., 2014). *NRT1.1* is a dual-affinity nitrate uptake protein whose phosphorylation at Thr101 by the protein kinase CIPK23 results in activation of the high-affinity transport mode of *NRT1.1* (Ho et al., 2009). Hence, we tested whether CIPK23 could also phosphorylate *NRT1.4*. The sequence alignment of *NRT1.1* and *NRT1.4* indicated that residue Thr98 at the head of the third

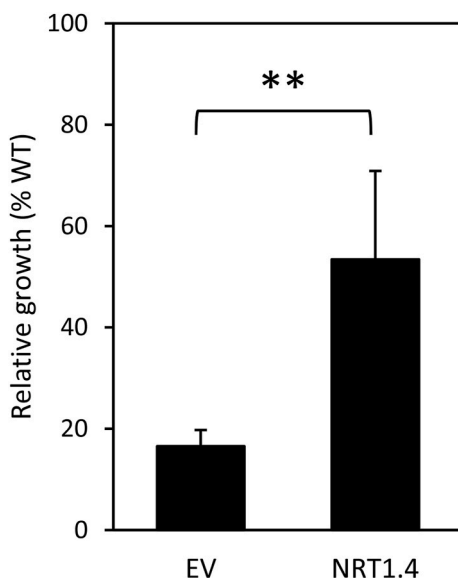


**Fig. 3.** *NRT1.4* expression in *H. polymorpha*. Single colonies of parental strain NCYC495 (*YNT1*), and of the  $\Delta ynt1$  mutant transformed with empty vector (EV) or with the cDNA encoding *NRT1.4* (*NRT1.4*) were grown 16h at 37 °C with shaking in YGNH medium. Millesimal dilutions of cell cultures at  $DO_{660} \sim 1$  were incubated in the same medium without nitrogen source (YG) plus 0.5 mM  $KNO_3$  for 48 h. Yeast growth were measured at  $DO_{660}$  and expressed as percent of growth relative to the control *YNT1* strain. Bars are mean and SD (EV,  $n = 3$ ; *NRT1.4*,  $n = 10$ ; all independent transformants). Asterisks indicate  $p < 0.01$  by *t*-test.

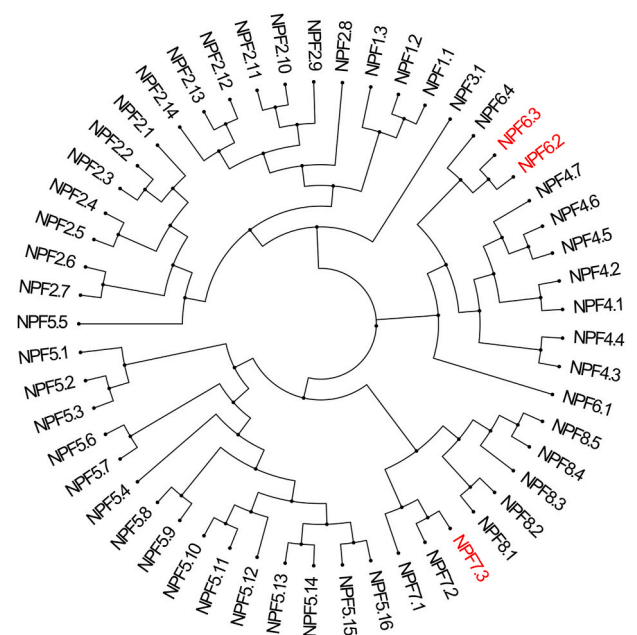


**Fig. 4.** Phylogenetic tree of the NPF protein family of *Arabidopsis thaliana*. Alignment of the 53 sequences from the NPF family was carried out by MUSCLE method. A graphical view of the tree was generated using FigTree. NPF6.3/*NRT1.1*, NPF6.2/*NRT1.4* and NPF7.3/*NRT1.5* are marked in red. (For interpretation of the references to color in this figure legend, the reader is referred to the Web version of this article.)

transmembrane domain (TM3) corresponded to Thr101 of *NRT1.1* (Fig. 5). A fragment of *NRT1.4* spanning from amino acids Phe92 to Phe102, and containing or not the mutation T98A, were fused to GST. Next, unmodified GST and both recombinant fusion proteins (GST-*NRT1.4* and GST-T98A) were recovered from bacteria a submitted to an *in vitro* phosphorylation assay as substrates for the hyperactive kinase CIPK23- $\Delta C$ -T190D. The wild-type CIPK23 protein is intrinsically inactive *in vitro*, but it can be activated by removal of the C-terminal autoinhibitory domain and the phospho-mimicking mutation T190D in the activation loop (Chaves-Sanjuan et al., 2014; Sanchez-Barrena et al., 2020). Results of the phosphorylation assays demonstrated that, as anticipated, CIPK23 phosphorylates *NRT1.4* at residue Thr98 (Fig. 5).

Co-expression of *NRT1.4* and CIPK23 in *Hansenula* to test activation of nitrate transport was an impractical approach. Firstly, the *ynt1* strain does not allow for the co-expression of multiple proteins due to the lack of sufficient transformation markers. Secondly, recruitment of CIPK23 to the plasma membrane in the vicinity of the target protein requires of the alternative interacting partners CBL1 or CBL9 that recruit the kinase to the membrane (Xu et al., 2006; Ho et al., 2009; Sanchez-Barrena et al., 2020), and expression of the recombinant hyperactive kinase CIPK23- $\Delta C$ -T190D alone could fail to activate *NRT1.4* *in vivo* if not properly targeted to the cell membrane. Therefore, to co-express *NRT1.4* with CIPK23/CBL1 we used *Xenopus* oocytes, which have been successfully used for the functional testing of NPF proteins (Corratgé-Faillie and Lacombe, 2017). We first attempted the electrophysiological approach described originally for measuring the nitrate transport activity of *NRT1.4* (Chiu et al., 2004). However, in our hands and despite multiple efforts, *NRT1.4* failed to produce measurable currents in oocytes by the two-electrode voltage-clamp method. Hence, we used instead the  $^{15}N$ -labeled nitrate accumulation method (Leran et al., 2015). In this assay, *NRT1.4* mediated measurable nitrate transport with and without the co-expression of CIPK23 and CBL1 (Fig. 6). Notably, the transport activity of *NRT1.4* in the low-affinity range (30 mM nitrate) was reduced by 34% in the presence of the CIPK23/CBL1 kinase complex.

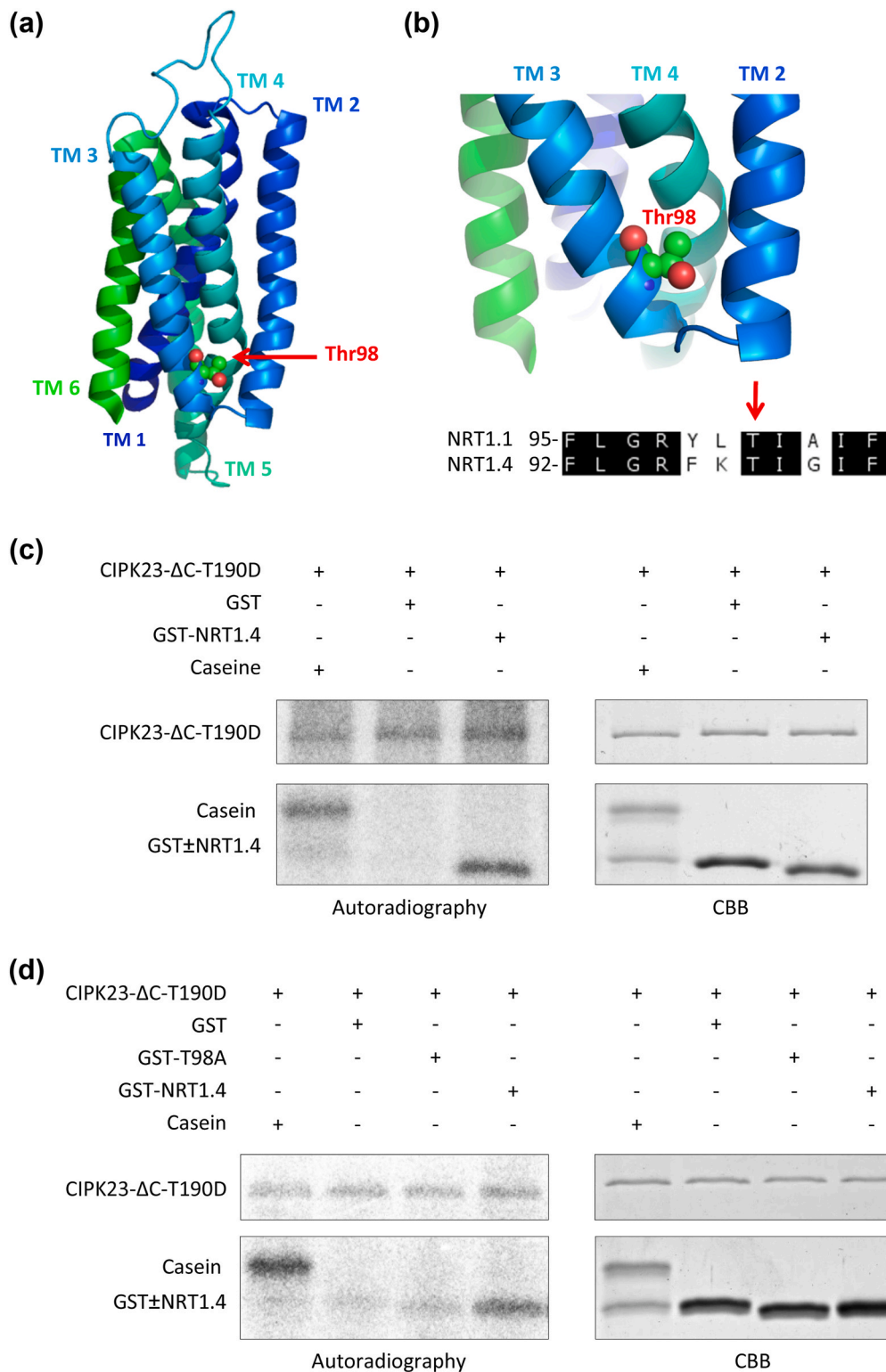


**Fig. 5.** CIPK23 phosphorylates NRT1.4 at Thr98. **(a)** Tridimensional structure of the pore domain NRT1.4, showing transmembrane segments 1 to 5 (TM1–TM5), modeled after the crystal structure of NRT1.1 (PDB code 4oh3B) using the Swiss-Model tool (<https://swissmodel.expasy.org>). Residue Thr98, localized in TM3, is represented as spheres. **(b)** Close-up view of Thr98 at the head of TM3 and alignment of amino acids of NRT1.1 and NRT1.4 around position Thr101 of NRT1.1, the target of CIPK23. **(c)** In vitro phosphorylation of NRT1.4 (region F92–F102 fused to GST) in the presence of  $[\gamma\text{-}^{32}\text{P}]\text{ATP}$  and the recombinant CIPK23-ΔC-T190D kinase. Casein and GST were used as phosphorylation controls. After the phosphorylation reactions, the proteins were separated by 12.5% SDS-PAGE and the incorporated radioactivity was analyzed by autoradiography (left panels). Coomassie Brilliant Blue (CBB) staining is shown in the right panels. The panels labeled as CIPK23-AC-T190D show the autophosphorylation of the kinase. **(d)** Similar experiment to that shown in (c) including a GST-NRT1.4 target protein fragment with mutation T98A (GST-T98A) to demonstrate the phosphorylation site by CIPK23. (For interpretation of the references to color in this figure legend, the reader is referred to the Web version of this article.)

### 3.3. NRT1.4 does not transport potassium

NPF proteins can transport a surprisingly wide variety of substrates, including nitrate, nitrite, peptides, amino acids, dicarboxylates, glucosinolates, IAA, and ABA (Corratgé-Faillie and Lacombe, 2017; Wang et al., 2018). Recently, family members NPF7.3/NRT1.5 and NPF7.2/NRT1.8 have been suggested to transport  $\text{K}^+$  (Li et al., 2017), although the precise transport mechanism remains uncertain (Raddatz

et al., 2020). This was an intriguing finding considering the extensive and intimate relationships between nitrate and  $\text{K}^+$  nutrition in plants (Raddatz et al., 2020). To explore whether NRT1.4 could use  $\text{K}^+$  as substrate or be co-transported with nitrate as counter-ion, we tested NRT1.4 activity in *S. cerevisiae* mutants defective in  $\text{K}^+$  uptake and efflux. NRT1.5 was also included in these experiments to confirm whether this protein could mediate  $\text{K}^+$ /nitrate co-transport.

We first tested nitrate-dependent  $\text{K}^+$  uptake in the yeast strain

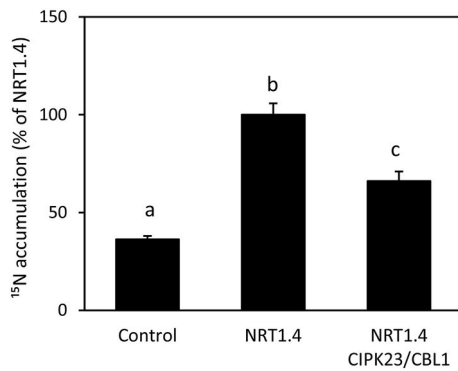


**Fig. 6.** <sup>15</sup>N-nitrate accumulation in *Xenopus* oocytes. Water-injected (Control), NRT1.4 and NRT1.4/CIPK23/CBL1-expressing oocytes were incubated with 30 mM <sup>15</sup>N-labeled nitrate. The <sup>14</sup>N/<sup>15</sup>N ratio was determined in dried oocytes. Data are mean and SEM (*n* = 8–9 oocytes). Letters indicate significant differences (*p* < 0.05) by ANOVA comparison with Tukey’s post-hoc test between NRT1.4-expressing oocytes with or without CIPK23/CBL1, and water-injected control oocytes.

TTE9.3 that is defective in the main K<sup>+</sup>-uptake system of this species (TRK1 and TRK2 proteins) and unable to grow at 0.1 mM K<sup>+</sup>. All genotypes grew normally at 50 mM KCl (Fig. 7). Expression of the K<sup>+</sup>-selective channel AKT1 mediating K<sup>+</sup> uptake in plant roots (Sentenac et al., 1992) suppressed the *trk1 trk2* mutant phenotype in K<sup>+</sup>-limiting conditions. However, NRT1.4 failed to restore growth of TTE9.3 cells in 0.1 mM K<sup>+</sup> and to improve growth at the intermediate selective concentration of 10 mM K<sup>+</sup> above the levels imparted by the empty-vector control. This failure occurred with and without the co-expression of CIPK23 and CBL1, and independently of whether K<sup>+</sup> was provided as chloride or nitrate salt. NRT1.5 produced the same results (Fig. 7). Together, these data indicate that neither NRT1.4 nor NRT1.5 mediate nitrate-dependent K<sup>+</sup> uptake in yeast cells.

We next tested whether NRT1.4 or NRT1.5 could mediate K<sup>+</sup> efflux. Both proteins were expressed, with and without CIPK23/CBL1, in the yeast strain AXT3K (*ena1-ena4, nha1, nhx1*) that lacks the (Na<sup>+</sup>,K<sup>+</sup>)-pumps ENA1 to ENA4 and the K<sup>+</sup>(Na<sup>+</sup>)/H<sup>+</sup> exchanger NHA1. These proteins reside at the plasma membrane, mediate K<sup>+</sup> efflux and are required to tolerate high external K<sup>+</sup> concentrations (Quintero et al., 2002). Again, neither NRT1.4 nor NRT1.5 produced a phenotype that departed from the empty-vector controls, with and without the co-expression of CIPK23 and CBL1 (Fig. 8). The AXT3K strain is also

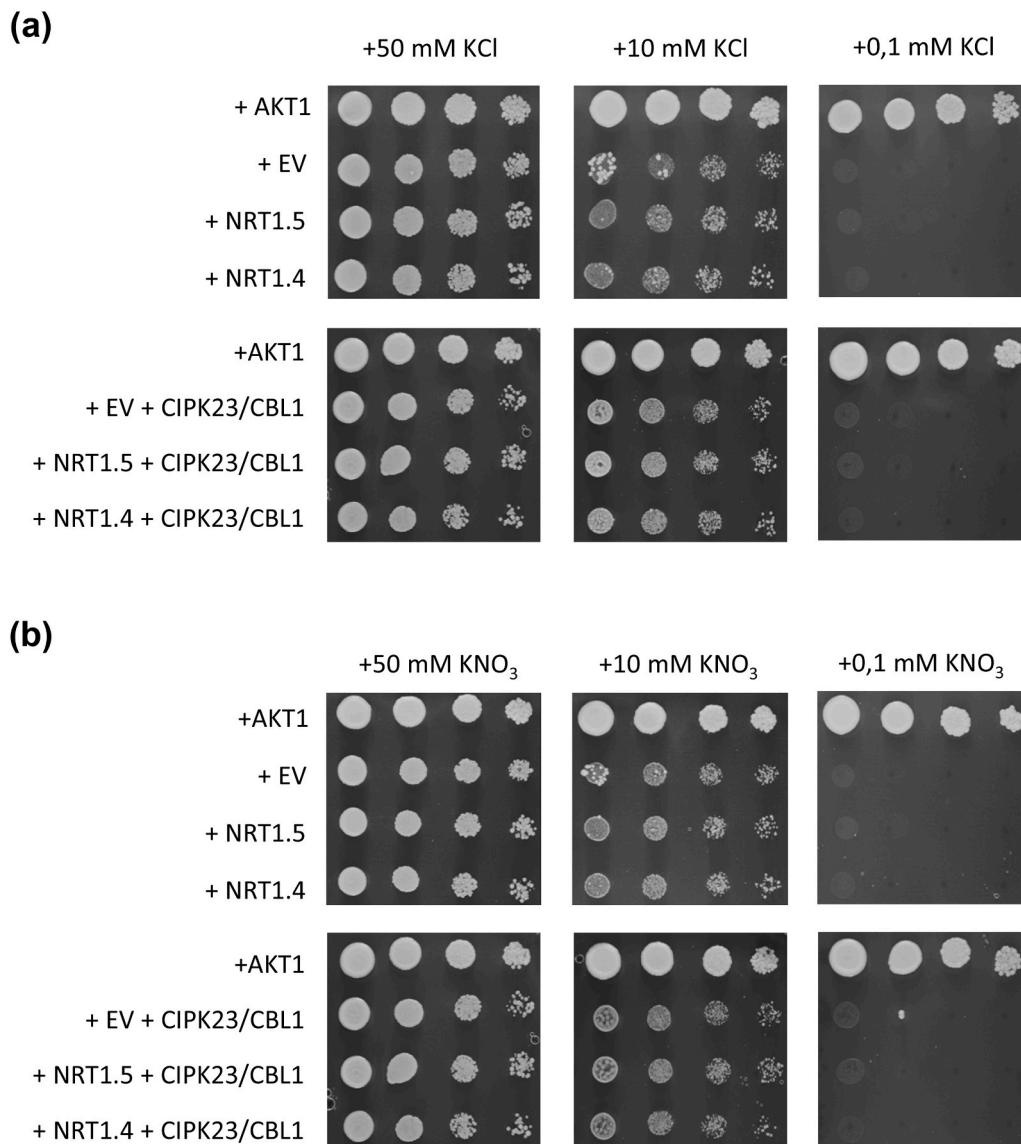


**Fig. 7.** Nitrate-dependent potassium uptake in *S. cerevisiae*. Cells of strain TTE9.3 (*trk1, trk2, ena1-4*) were transformed with de empty vector (EV) or the indicated combination of cDNAs encoding AKT1, NRT1.4, NRT1.5, CIPK23 and CBL1. Yeast transformants were grown overnight in medium with 50 mM KCl. Five microliters of serial decimal dilutions were spotted onto plates of AP medium supplemented with the indicated KCl (a) or KNO<sub>3</sub> (b) concentration, and then they were incubated at 28 °C for 3–4 days.

(a)

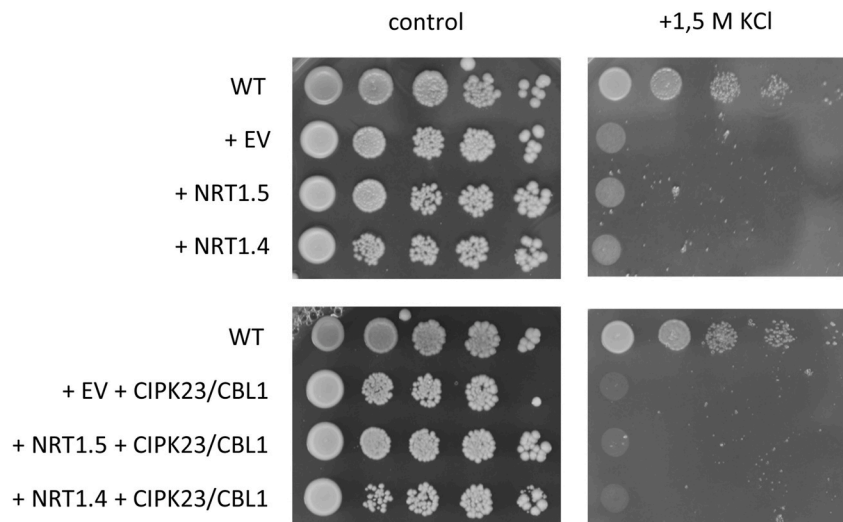
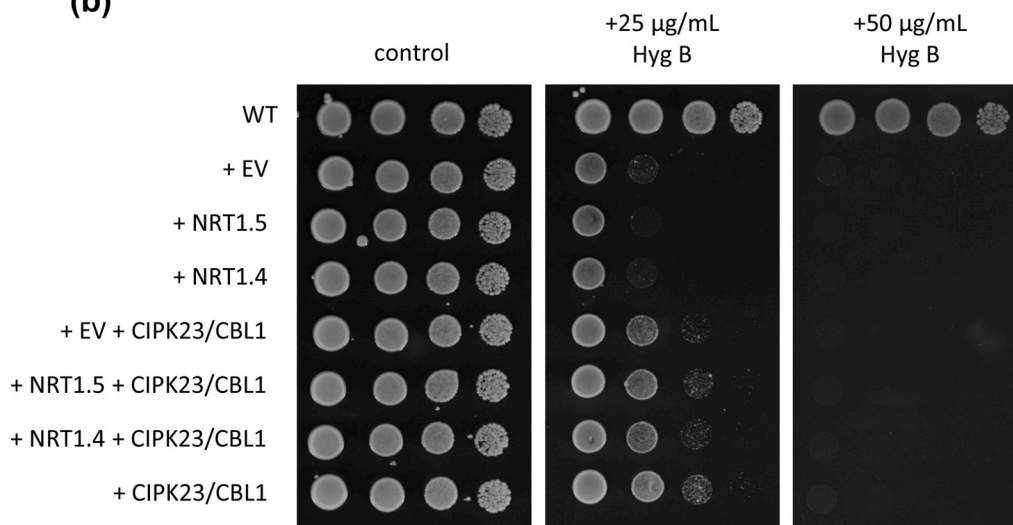


**Fig. 8.** Potassium efflux in *S. cerevisiae*. Cells of strain AXT3K (*ena1-4*, *nha1*, *nhx1*) were transformed with the empty vector (EV) or the indicated combination of cDNAs encoding NRT1.4, NRT1.5, CIPK23 and CBL1. Strain W303 was used as positive control (WT). Yeast transformants were grown overnight in YPD medium. Five microliters of serial decimal dilutions were spotted onto plates of YPD medium buffered to pH 5.5 and supplemented with the indicated concentration of KCl (a) or hygromycin B (b), and then they were incubated at 28 °C for 3 days.

(b)



missing the  $\text{Na}^+/\text{K}^+/\text{H}^+$  exchanger NHX1 at the vacuole and pre-vacuolar compartment, which translates in sensitivity to hygromycin B (Hernandez et al., 2009). When expressed alone, neither NRT1.4 nor NRT1.5 modified the sensitivity to the antibiotic. Co-expression of CIPK23 and CBL1 produced partial resistance to hygromycin B, but this was not related to NRT1.4 and NRT1.5 expression because the increment was also observed in the empty-vector control without NRT1.4 and NRT1.5, or when the CIPK23-CBL1 complex was transformed alone. The target(s) of CIPK23-CBL1 in the yeast *S. cerevisiae* that alter the sensitivity to hygromycin B are unknown. The negative results of the  $\text{K}^+$ -transport assay in *S. cerevisiae* could not be attributed to no expression or missorting of the NRT1.4 protein because the NRT1.4-GFP translational fusion produced fluorescence arising from both the cell surface and the central vacuole (Fig. 9), thereby confirming that the recombinant protein reached the intended cellular membranes. In summary, no effect of NRT1.4 and NRT1.5 transporters could be observed in  $\text{K}^+$  fluxes in the yeast *S. cerevisiae*, whether for uptake, efflux or vacuolar compartmentation.

#### 4. Discussion

The *Arabidopsis* protein NPF6.2/NRT1.4 has been previously described as a proton-dependent nitrate uptake protein, gating nitrate flux at the leaf petiole to regulate leaf nitrate metabolism (Chiu et al., 2004). We have confirmed the reduced nitrate content in the leaf petiole of a loss-of-function *nrt1.4* mutant plant (Fig. 2a) but could not find differences in the nitrate contents in leaf lamina, or in whole shoots and roots of *nrt1.4* compared to the wild-type under two nitrate availability regimes (0.5 and 4 mM). However, NRT1.4 is also expressed, in decreasing order of mRNA abundance, in guard cells, root pericycle, stem nodes and shoot vascular tissue (<https://genevisible.com/tissues/AT/Ensembl%20Gene/AT2G26690>). This wide expression pattern could confer additional roles to NRT1.4 in plant physiology. Indeed, we observed increased  $\text{K}^+$  content in the shoots of the *nrt1.4* mutant grown in 1 mM  $\text{K}^+$  and 4 mM  $\text{NO}_3^-$  (Fig. 2d), but reduced  $\text{K}^+$  content in the mutant root under low  $\text{NO}_3^-$  supply (0.5 mM, Fig. 2f). These results evidence the impact of NRT1.4 function in roots and suggest a role for NRT1.4 in  $\text{K}^+$  nutrition in our experimental conditions. These differences in  $\text{K}^+$  contents could still be due to altered nitrate transport

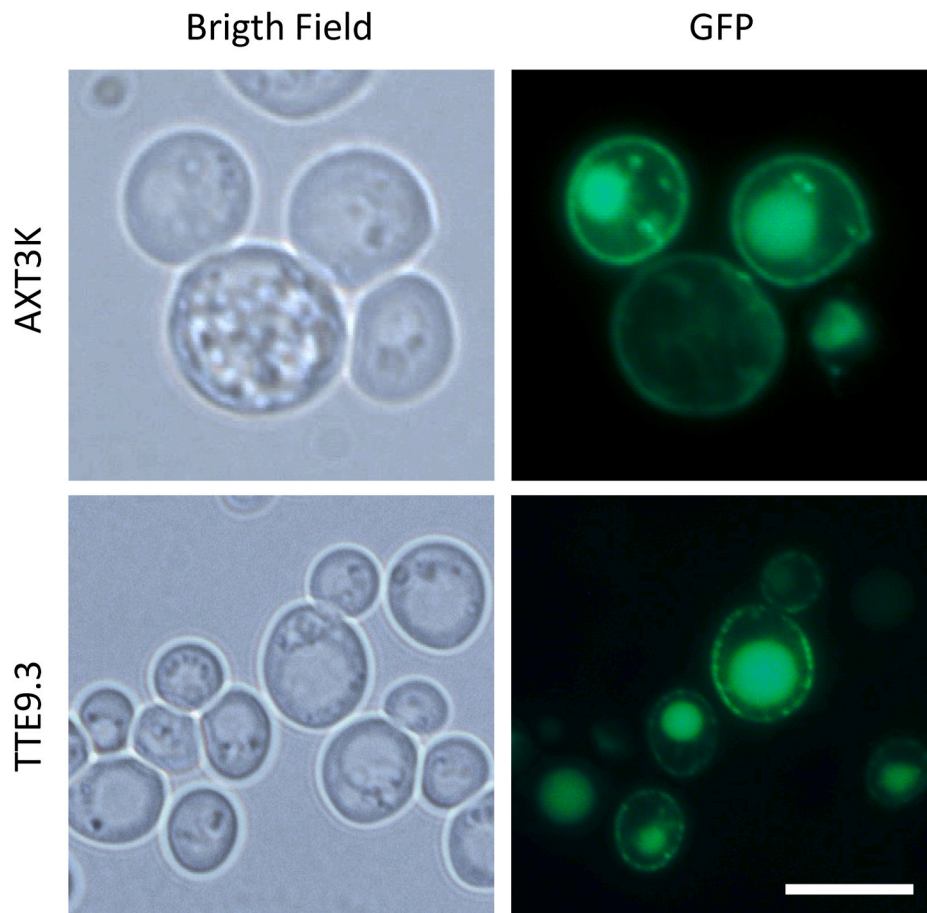


Fig. 9. Subcellular localization of GFP-tagged NRT1.4 in *S. cerevisiae*. Epifluorescence microscopy of cells AXT3K and TTE9.3 transformed with NRT1.4-GFP and grown 24 h in YPD media at 28 °C. Left, bright field; right, GFP fluorescence. Fluorescence was predominant in plasma membrane and vacuoles. Scale bar is 5  $\mu$ m.

because of the intimate relationship between these nutrients in *Arabidopsis* (Raddatz et al., 2020; references therein). Plants can sense  $K^+$  and  $NO_3^-$  levels and adjust the uptake and root-to-shoot transport to balance the distribution of these ions between organs. In most plant species, the uptake of  $K^+$  and  $NO_3^-$  from the soil and their distribution throughout the plant organs and tissues are positively correlated. This correlative effect has been attributed to improved charge balance during nutrient uptake and long-distance transport. NRT1.4 has been suggested to re-absorb nitrate at the petiole and restrict the flux to the lamina (Chiu et al., 2004). The large reduction of the nitrate content in the petiole of the *nrt1.4* mutant at 4 mM  $NO_3^-$  (Fig. 2a) is in agreement with this notion. A greater nitrate flux into the leaves of *nrt1.4* could drive enhanced  $K^+$  accumulation in aerial tissues (Fig. 2d). Likewise, compromised nitrate uptake in the *nrt1.4* mutant could translate into reduced  $K^+$  content in the mutant root when nitrate was reduced to 0.5 mM (Fig. 2f). This suggests a positive effect of NRT1.4 on  $K^+$  transport at low-nitrate supply to ensure sufficient  $K^+$  acquisition. That changes in nitrate contents in shoot and roots of *nrt1.4* plants were not commensurate with those of  $K^+$  could reflect nitrate assimilation into organic matter, which is a distinctive feature of nitrate over  $K^+$ . In other words, nitrate assimilation could have cancelled small differences in the nitrate contents in these organs.

At least three other *Arabidopsis* NPF proteins, NPF6.3/NRT1.1, NPF7.3/NRT1.5 and NPF7.2/NRT1.8, are known to impinge on  $K^+$  nutrition. Intriguingly, NPF7.3/NRT1.5 and NPF7.2/NRT1.8 seem capable of transporting  $K^+$  (Li et al., 2017). However, nitrate is not only a primary nitrogen source, but also serves as a signaling molecule to plants (Wang et al., 2018, 2021), and the nitrate-sensor NPF6.3/NRT1.1 is required for plant growth under  $K^+$ -limiting conditions (Fang et al.,

2020). Alike the *nrt1.4* mutant, *nrt1.1* plants show disturbed  $K^+$  root-to-shoot allocation. Double mutant analyses revealed physiological interactions between NPF6.3/NRT1.1 and root  $K^+$  transporters that were dependent on  $H^+$ -consumption associated with the  $H^+/NO_3^-$  symport mediated by NPF6.3/NRT1.1, which in turn affected the operation of  $K^+$  channels and transporters (Fang et al., 2020). Our data signify that NPF6.2/NRT1.4 adds to the growing list of nitrate transporters affecting  $K^+$  nutrition.

Moreover, NPF6.2/NRT1.4 is the closest homolog of NPF6.3/NRT1.1 in the NPF family of *Arabidopsis* (Fig. 4) and retains conserved amino acids equivalent to two key residues of NRT1.1, Pro492 and Thr101 (Bougyon et al., 2015; Maghiaoui et al., 2020). The P492L mutation de-couples nitrate transport from the nitrate-sensing role of NRT1.1, whereas the phosphorylation status of Thr101 switches the low- and high-affinity transport mode and controls the repressive role of NRT1.1 in the Primary Nitrate Response (PNR) (Liu and Tsay, 2003; Ho et al., 2009; Bougyon et al., 2015). Considering the similarities to NPF6.3/NRT1.1 and that the *nrt1.4* mutant plant had disturbed  $K^+$  partition, protein NRT1.4 merited a deeper characterization in terms of subcellular localization, transported substrate(s) and phosphorylation by CIPK23. Through the heterologous expression of NRT1.4 in four expression systems, namely *N. benthamiana*, *H. polymorpha*, *S. cerevisiae* and *Xenopus* oocytes, we have shown that NRT1.4 is a plasma membrane protein endowed with nitrate transport capability in the millimolar range (0.5 and 30 mM nitrate in yeast and oocytes, respectively). We also tested whether NRT1.4 transported  $K^+$  or displayed nitrate-dependent  $K^+$  uptake, with negative results in both instances. NRT1.5 affects root-to-shoot  $K^+$  translocation under low-nitrate conditions (Drechsler et al., 2015), influences the transport of  $K^+$  and nitrate

via xylem under limiting  $K^+$  (Li et al., 2017), and has been suggested to catalyze  $H^+/K^+$  exchange for  $K^+$  loading into the xylem in *Arabidopsis*. Hence, we compared the activity of NRT1.4 to that of NRT1.5 in terms of  $K^+$  transport using the well-established *S. cerevisiae* system for the assay of plant  $K^+$  transporters (Yenush, 2016; Ródenas et al., 2021). However, NRT1.5 failed to produce any discernible phenotype in yeast mutants impaired in  $K^+$  uptake, using both KCl and  $KNO_3$  salts as substrate, or defective in  $K^+$  efflux and vacuolar compartmentation (Figs. 7 and 8). It should be noted, however, that Li et al. (2017) did not conduct growth complementation tests; instead they compared the rate of  $K^+$  loss in  $K^+$ -free medium in yeast cell expressing NRT1.5, a dead NRT1.5 protein with mutation G209E, and empty-vector control. The rate of  $K^+$ -loss in NRT1.5 cells was only slightly higher than that of negative controls, which also released  $K^+$  over time. Our negative results confirm and extend those of Drechsler et al. (2015), but do not preclude that NRT1.5 may indeed facilitate the release of  $K^+$  under a favorable outward-directed  $K^+$  gradient across the plasma membrane as in Li et al. (2017). Instead, our results indicate that NRT1.5 is incapable of promoting  $K^+$  efflux when the  $K^+$  gradient is directed inwards and energized by the inward-directed proton motive force, as would be expected from a  $K^+/H^+$  exchanger. On the other hand, the mutant complementation  $K^+$ -uptake assay in *trk1 trk2* cells of *S. cerevisiae* is a highly sensitive test, owing to a large inward-directed  $K^+$  gradient and the plasma membrane hyperpolarization, negative inside, of *trk1 trk2* cells (Yenush, 2016). In this assay, both NRT1.4 and NRT1.5 failed to demonstrate  $K^+$  influx. In summary, it is unlikely that NRT1.4 facilitates  $K^+$  transport, not even in co-transport with nitrate (Fig. 7).

Analysis of the crystal structure of nitrate-bound NRT1.1 indicated that residue His326 was important for nitrate coordination, as mutation of this residue resulted in the loss of nitrate binding and transport (Parker and Newstead, 2014; Sun et al., 2014). However, members of the NPF family display substantial amino acidic variability at this position, and histidine is present in only three members, NPF6.3/NRT1.1, NPF8.4 and NPF5.11. The equivalent residues are Tyr346 in NRT1.4, also transporting nitrate, and Phe367 and Phe354 in NRT1.5 and NRT1.8, which could transport  $K^+$ . On the other hand, the conserved motif ExxERF on TM1 is important for proton coupling and nitrate/proton symport by NRT1.1 (Sun et al., 2014). This motif is found in all NPF/NRT1 family members but NRT1.5 and NRT1.8, suggesting that their nitrate transport activity initially reported necessitated an alternative cation-coupling energizing mechanism (Sun et al., 2014). Theoretically, the monovalent cation  $K^+$  could fulfill this coupling role in a hypothetical  $K^+$ /nitrate co-transport by NRT1.5, but our negative results regarding the nitrate-dependent  $K^+$  uptake in *trk1 trk2* cells (Fig. 7) do not support this possibility, which could have explained the intimate relation between  $K^+$  and nitrate transport associated to NRT1.5 function. The structural determinants enabling the  $K^+/H^+$  exchange mechanism of NRT1.5 and NRT1.8 remain unexplained and deserve further experimentation.

An interesting result is that CIPK23 phosphorylates NRT1.4 at residue Thr98, which is equivalent to the Thr101 phosphorylation site of NRT1.1. Phosphorylation by CIPK23 triggers the toggling between low- and high-affinity modes of nitrate uptake by NRT1.1 (Liu and Tsay, 2003), albeit how this post-translational modification switches the transporter between two affinity states remains unclear. The crystal structure of NRT1.1 reveals a homodimer, and the dynamic assembly and disassembly of protomers controlled by the phosphorylation status of Thr101 (Sun et al., 2014). The structural engagement of two protomers could regulate allosterically the affinity of substrate binding, being the monomer responsible for the high-affinity transport mode (Sun et al., 2014). However (Rashid et al., 2020), proposed an alternative sequence of events by which nitrate binding at the high-affinity site initiates NRT1.1 dimer decoupling, thereby priming the previously buried Thr101 site for phosphorylation by CIPK23. In this model, phosphorylation stabilizes the NRT1.1 monomer acting as a high-affinity nitrate transporter. Regardless of the precise structural

mechanism involved in the kinetic transition, phosphorylation of NRT1.1 enables high-affinity transport, presumably at the expense of reduced transport rate in the low-affinity (mM) range (Liu and Tsay, 2003). Our results with the co-expression of NRT1.4 and CIPK23/CBL1 in *Xenopus* oocytes show reduced transport at 30 mM external nitrate, i. e. the low-affinity range (Fig. 6). Owing to the low transport rate by NRT1.4, we could not measure reliably nitrate uptake by NRT1.4 in the  $\mu$ M range of substrate. In our hands, NRT1.4 was electrically silent in oocytes, which could be due to electroneutral nitrate/proton symport by NRT1.4. Chiu et al. (2004) reported NRT1.4-dependent nitrate-inward currents by the two-electrode voltage-clamp (TEVC) method, but technical glitches when measuring nitrate fluxes by TEVC in *Xenopus* oocytes have been reported (Noguero et al., 2018). In summary, our results demonstrate that CIPK23 phosphorylates NRT1.4 at Thr98, and that this modification reduces the transport rate of NRT1.4 in the low-affinity range. Based on the lower  $K^+$  content in the root of the loss-of-function mutant *nrt1.4* at low external nitrate (Fig. 2f), and the known role of CIPK23 to stimulate  $K^+$  uptake and to regulate nitrate transport (Leran et al., 2015; Ragel et al., 2015, 2019; Ródenas and Vert, 2021) we speculate that the reduced nitrate transport by NRT1.4 upon co-expression with CIPK23/CBL1 in oocytes may reflect the need to re-adjust nitrate transport and  $K^+$  uptake systems to fine tune the co-transport of these nutrients to maintain electroneutrality.

## 5. Conclusions

Here we have shown that NPF6.2/NRT1.4 is a plasma membrane protein mediating nitrate uptake in the millimolar, low-affinity range, and also a target of the protein kinase CIPK23 that regulates the response of plants to limited  $K^+$  and nitrate availability. Despite the noticeable effects that NPF6.2/NRT1.4 and NPF7.3/NRT1.5 have in the transport and nutrition of  $K^+$ , we could find no evidence of nitrate-dependent  $K^+$  fluxes mediated by NRT1.4 or NRT1.5.

## Author contributions

LMR determined NRT1.4 subcellular localization in plants and yeast. LMR, IM and FJQ conducted experiments with the yeast *H. polymorpha* and *S. cerevisiae*. LMR, CCF and NR measured NRT1.4 activity in *Xenopus* oocytes. LMR and ML did the phosphorylation assays. AA, BL, FJQ and JMP designed the research. LMR and JMP wrote the paper.

## Funding

This work was supported by Agencia Estatal de Investigación (AEI-MCIU, Spain), co-financed by the European Regional Development Fund (grants RTI 2018-094027-B-100 to JMP, and PID 2019-109664-RB-100 to FJQ), by Agence Nationale de la Recherche (ANR-HONIT to BL) and by Centre National de la Recherche Scientifique (ATIP-AVENIR-2018 program to ADA).

## Declaration of competing interest

The authors declare that they have no known competing financial interests or personal relationships that could have appeared to influence the work reported in this paper.

## Acknowledgements

We are thankful to Prof. J.M Siverio (Universidad de La Laguna) for the *Hansenula* strains and expression vector, to Prof. Yi Wang (China Agricultural University) for the NRT1.5 plasmid, to Prof. J. Kudla (Munster University) for the CBL1-OPF plasmid, and to Dr. F.J. Perez-Hormaeche and Alicia Orea (IBVF-CSIC) for assistance with confocal microscopy.

## References

- Bañuelos, M.A., Klein, R.D., Alexander-Bowman, S.J., Rodríguez-Navarro, A., 1995. A potassium transporter of the yeast *Schwanniomyces occidentalis* homologous to the Kup system of *Escherichia coli* has a high concentrative capacity. *EMBO J.* 14, 3021–3027. <https://doi.org/10.1002/j.1460-2075.1995.tb07304.x>.
- Barragan, V., Leidi, E., Andres, Z., Rubio, L., De Luca, A., Fernandez, J., et al., 2012. Ion exchangers NHX1 and NHX2 mediate active potassium uptake into vacuoles to regulate cell turgor and stomatal function in *Arabidopsis*. *Plant Cell* 24, 1127–1142. <https://doi.org/10.1105/tpc.111.095273>.
- Batistic, O., Sorek, N., Schultke, S., Yalovsky, S., Kudla, J., 2008. Dual fatty acyl modification determines the localization and plasma membrane targeting of CBL/CIPK Ca<sup>2+</sup> signaling complexes in *Arabidopsis*. *Plant Cell* 20 (5), 1346–1362. <https://doi.org/10.1105/tpc.108.058123>.
- Bouguyon, E., Brun, F., Meynard, D., Kubes, M., Pervent, M., Leran, S., et al., 2015. Multiple mechanisms of nitrate sensing by *Arabidopsis* nitrate transporter NRT1.1. *Native Plants* 1, 15015. <https://doi.org/10.1038/nplants.2015.15>.
- Brunelli, J.P., Pall, M.L., 1993. A series of yeast shuttle vectors for expression of cDNAs and other DNA sequences. *Yeast* 9 (12), 1299–1308. <https://doi.org/10.1002/yea.320091203>.
- Cataldo, D.A., Maroon, M., Schrader, L.E., Youngs, V.L., 1975. Rapid colorimetric determination of nitrate in plant tissue by nitration of salicylic acid. *Commun. Soil Sci. Plant Anal.* 6 (1), 71–80. <https://doi.org/10.1080/00103627509366547>.
- Chaves-Sanjuan, A., Sanchez-Barrena, M.J., Gonzalez-Rubio, J.M., Moreno, M., Ragel, P., Jimenez, M., et al., 2014. Structural basis of the regulatory mechanism of the plant CIPK family of protein kinases controlling ion homeostasis and abiotic stress. *Proceedings of the National Academy of Sciences USA* 111 (42), E4532–E4541. <https://doi.org/10.1073/pnas.1407610111>.
- Chiu, C.C., Lin, C.S., Hsia, A.P., Su, R.C., Lin, H.L., Tsay, Y.F., 2004. Mutation of a nitrate transporter, *AtNRT1.4*, results in a reduced petiole nitrate content and altered leaf development. *Plant Cell Physiol.* 45 (9), 1139–1148. <https://doi.org/10.1093/pcp/pch143>.
- Corratgé-Faillie, C., Lacombe, B., 2017. Substrate (un)specificity of *Arabidopsis* NRT1/PTR FAMILY (NPF) proteins. *J. Exp. Bot.* 68 (12), 3107–3113. <https://doi.org/10.1093/jxb/erw499>.
- Drechsler, N., Zheng, Y., Bohner, A., Nobmann, B., von Wiren, N., Kunze, R., et al., 2015. Nitrate-dependent control of shoot K homeostasis by the nitrate transporter1/peptide transporter family member NPF7.3/nrt1.5 and the stelar K<sup>+</sup> outward rectifier SKOR in *Arabidopsis*. *Plant Physiol.* 169 (4), 2832–2847. <https://doi.org/10.1104/pp.15.01152>.
- Fang, X.Z., Liu, X.X., Zhu, Y.X., Ye, J.Y., Jin, C.W., 2020. The K<sup>(+)</sup> and NO<sub>3</sub><sup>(-)</sup> interaction mediated by NITRATE TRANSPORTER1.1 ensures better plant growth under K<sup>(+)</sup>-limiting conditions. *Plant Physiol.* 184 (4), 1900–1916. <https://doi.org/10.1104/pp.20.01229>.
- Geiger, D., Scherzer, S., Mumm, P., Stange, A., Marten, I., Bauer, H., et al., 2009. Activity of guard cell anion channel SLAC1 is controlled by drought-stress signaling kinase-phosphatase pair. *Proc. Natl. Acad. Sci. U. S. A.* 106 (50), 21425–21430. <https://doi.org/10.1073/pnas.0912021106>.
- Gietz, R.D., Schiestl, R.H., 2007. Quick and easy yeast transformation using the LiAc/SS carrier DNA/PEG method. *Nat. Protoc.* 2 (1), 35–37. <https://doi.org/10.1038/nprot.2007.14>.
- Harper, S., Speicher, D.W., 2008. Expression and purification of GST fusion proteins. In: *Current Protocols in Protein Science*.
- Held, K., Pascaud, F., Eckert, C., Gajdanowicz, P., Hashimoto, K., Corratgé-Faillie, C., et al., 2011. Calcium-dependent modulation and plasma membrane targeting of the AKT2 potassium channel by the CBL4/CIPK6 calcium sensor/protein kinase complex. *Cell Res.* 21 (7), 1116–1130. <https://doi.org/10.1038/cr.2011.50>.
- Hernandez, A., Jiang, X., Cubero, B., Nieto, P.M., Bressan, R.A., Hasegawa, P.M., et al., 2009. Mutants of the *Arabidopsis thaliana* cation/H<sup>+</sup> antiporter *AtNHX1* conferring increased salt tolerance in yeast: the endosome/prevacuolar compartment is a target for salt toxicity. *J. Biol. Chem.* 284 (21), 14276–14285. <https://doi.org/10.1074/jbc.M806203200>.
- Ho, C.H., Lin, S.H., Hu, H.C., Tsay, Y.F., 2009. CHL1 functions as a nitrate sensor in plants. *Cell* 138 (6), 1184–1194. <https://doi.org/10.1016/j.cell.2009.07.004>.
- Lacombe, B., Thibaud, J.B., 1998. Evidence for a multi-ion pore behavior in the plant potassium channel KAT1. *J. Membr. Biol.* 166 (2), 91–100. <https://doi.org/10.1007/s002329900451>.
- Leran, S., Edel, K.H., Pervent, M., Hashimoto, K., Corratgé-Faillie, C., Offenborn, J.N., et al., 2015. Nitrate sensing and uptake in *Arabidopsis* are enhanced by ABI2, a phosphatase inactivated by the stress hormone abscisic acid. *Sci. Signal.* 8 (375), ra43. <https://doi.org/10.1126/scisignal.aaa4829>.
- Léran, S., Garg, B., Boursiac, Y., Corratgé-Faillie, C., Brachet, C., Tillard, P., et al., 2015. *AtNPF5.5*, a nitrate transporter affecting nitrogen accumulation in *Arabidopsis* embryo. *Sci. Rep.* 5, 7962. <https://doi.org/10.1038/srep07962>.
- Leran, S., Varala, K., Boyer, J.C., Chiu, R., Crawford, N., Daniel-Vedele, F., et al., 2014. A unified nomenclature of NITRATE TRANSPORTER 1/PEPTIDE TRANSPORTER family members in plants. *Trends Plant Sci.* 19 (1), 5–9. <https://doi.org/10.1016/j.tplants.2013.08.008>.
- Li, H., Yu, M., Du, X.Q., Wang, Z.F., Wu, W.H., Quintero, F.J., et al., 2017. NRT1.5/NPF7.3 functions as a proton-coupled H<sup>(+)</sup>/K<sup>(+)</sup> antiporter for K<sup>(+)</sup> loading into the xylem in *Arabidopsis*. *Plant Cell* 29 (8), 2016–2026. <https://doi.org/10.1105/tpc.16.00972>.
- Li, J.Y., Fu, Y.L., Pike, S.M., Bao, J., Tian, W., Zhang, Y., et al., 2010. The *Arabidopsis* nitrate transporter NRT1.8 functions in nitrate removal from the xylem sap and mediates cadmium tolerance. *Plant Cell* 22 (5), 1633–1646. <https://doi.org/10.1105/tpc.110.075242>.
- Lin, S.H., Kuo, H.F., Canivenc, G., Lin, C.S., Lepetit, M., Hsu, P.K., et al., 2008. Mutation of the *Arabidopsis* NRT1.5 nitrate transporter causes defective root-to-shoot nitrate transport. *Plant Cell* 20 (9), 2514–2528. <https://doi.org/10.1105/tpc.108.060244>.
- Liu, K.H., Tsay, Y.F., 2003. Switching between the two action modes of the dual-affinity nitrate transporter CHL1 by phosphorylation. *EMBO J.* 22 (5), 1005–1013. <https://doi.org/10.1093/emboj/cdg118>.
- Ma, L., Ye, J., Yang, Y., Lin, H., Yue, L., Luo, J., et al., 2019. The SOS2-SCaBP8 complex generates and fine-tunes an *AtANN4*-dependent calcium signature under salt stress. *Dev. Cell* 48 (5), 697–709. <https://doi.org/10.1016/j.devcel.2019.02.010>.
- Maghiaoui, A., Gojon, A., Bach, L., 2020. NRT1.1-centered nitrate signaling in plants. *J. Exp. Bot.* 71 (20), 6226–6237. <https://doi.org/10.1093/jxb/eraa361>.
- Martin, Y., Navarro, F.J., Siverio, J.M., 2008. Functional characterization of the *Arabidopsis thaliana* nitrate transporter CHL1 in the yeast *Hansenula polymorpha*. *Plant Mol. Biol.* 68 (3), 215–224. <https://doi.org/10.1007/s11103-008-9363-z>.
- Meng, S., Peng, J.S., He, Y.N., Zhang, G.B., Yi, H.Y., Fu, Y.L., et al., 2016. *Arabidopsis* NRT1.5 mediates the suppression of nitrate starvation-induced leaf senescence by modulating foliar potassium level. *Mol. Plant* 9 (3), 461–470. <https://doi.org/10.1016/j.molp.2015.12.015>.
- Nakamura, S., Mano, S., Tanaka, Y., Ohnishi, M., Nakamori, C., Araki, M., et al., 2010. Gateway binary vectors with the bialaphos resistance gene, bar, as a selection marker for plant transformation. *Biosci. Biotechnol. Biochem.* 74 (6), 1315–1319. <https://doi.org/10.1271/bbb.100184>.
- Noguero, M., Lacombe, B., 2016. Transporters involved in root nitrate uptake and sensing by *Arabidopsis*. *Front. Plant Sci.* 7, 1391. <https://doi.org/10.3389/fpls.2016.01391>.
- Noguero, M., Léran, S., Bouguyon, E., Brachet, C., Tillard, P., Nacry, P., et al., 2018. Revisiting the functional properties of NPF6.3/NRT1.1/CHL1 in xenopus oocytes. *bioRxiv* 244467. <https://doi.org/10.1101/244467>.
- Nour-Eldin, H.H., Hansen, B.G., Norholm, M.H., Jensen, J.K., Halkier, B.A., 2006. Advancing uracil-excision based cloning towards an ideal technique for cloning PCR fragments. *Nucleic Acids Res.* 34 (18), e122. <https://doi.org/10.1093/nar/gkl635>.
- Parker, J.L., Newstead, S., 2014. Molecular basis of nitrate uptake by the plant nitrate transporter NRT1.1. *Nature* 507 (7490), 68–72. <https://doi.org/10.1038/nature13116>.
- Pérez, M.D., González, C., Ávila, J., Brito, N., Siverio, J.M., 1997. The YNT1 gene encoding the nitrate transporter in the yeast *Hansenula polymorpha* is clustered with genes YNI and YNR1 encoding nitrite reductase and nitrate reductase, and its disruption cause inability to grow in nitrate. *Biochem. J.* 321, 397–403. <https://doi.org/10.1042/bj3210397>.
- Quintero, F.J., Ohta, M., Shi, H.Z., Zhu, J.K., Pardo, J.M., 2002. Reconstitution in yeast of the *Arabidopsis* SOS signaling pathway for Na<sup>+</sup> homeostasis. *Proceedings of the National Academy of Sciences USA* 99 (13), 9061–9066. <https://doi.org/10.1073/pnas.132092099>.
- Raddatz, N., Morales de los Ríos, L., Lindahl, M., Quintero, F.J., Pardo, J.M., 2020. Coordinated transport of nitrate, potassium, and sodium. *Front. Plant Sci.* 11, 247. <https://doi.org/10.3389/fpls.2020.00247>.
- Ragel, P., Raddatz, N., Leidi, E.O., Quintero, F.J., Pardo, J.M., 2019. Regulation of K<sup>(+)</sup> nutrition in plants. *Front. Plant Sci.* 10, 281. <https://doi.org/10.3389/fpls.2019.00281>.
- Ragel, P., Rodenas, R., Garcia-Martin, E., Andres, Z., Villalta, I., Nieves-Cordones, M., et al., 2015. The CBL-interacting protein kinase CIPK23 regulates HAK5-mediated high-affinity K<sup>+</sup> uptake in *Arabidopsis* roots. *Plant Physiol.* 169 (4), 2863–2873. <https://doi.org/10.1104/pp.15.01401>.
- Rashid, M., Bera, S., Banerjee, M., Medvinsky, A.B., Sun, G.Q., Li, B.L., et al., 2020. Feedforward control of plant nitrate transporter NRT1.1 biphasic adaptive activity. *Biophys. J.* 118 (4), 898–908. <https://doi.org/10.1016/j.bpj.2019.10.018>.
- Ródenas, R., Ragel, P., Nieves-Cordones, M., Martínez-Martínez, A., Amo, J., Lara, A., et al., 2021. Insights into the mechanisms of transport and regulation of the *Arabidopsis* high-affinity K<sup>+</sup> transporter HAK5. *Plant Physiol.* 185, 1860–1874. <https://doi.org/10.1093/plphys/kiab028>.
- Ródenas, R., Vert, G., 2021. Regulation of root nutrient transporters by CIPK23: 'one kinase to rule them all'. *Plant Cell Physiol.* 62 (4), 553–563. <https://doi.org/10.1093/pcp/pcaa156>.
- Rodríguez-Navarro, A., Ramos, J., 1984. Dual system for potassium transport in *Saccharomyces cerevisiae*. *J. Bacteriol.* 159 (3), 940–945. <https://doi.org/10.1128/jb.159.3.940-945.1984>.
- Sanchez-Barrena, M.J., Chaves-Sanjuan, A., Raddatz, N., Mendoza, I., Cortes, A., Gago, F., et al., 2020. Recognition and activation of the plant AKT1 potassium channel by the kinase CIPK23. *Plant Physiol.* 182 (4), 2143–2153. <https://doi.org/10.1104/pp.19.01084>.
- Sentenac, H., Bonneaud, N., Minet, M., Lacroute, F., Salmon, J.M., Gaymard, F., et al., 1992. Cloning and expression in yeast of a plant potassium ion transport system. *Science* 256 (5057), 663–665. <https://doi.org/10.1126/science.1585180>.
- Siverio, J.M., 2002. Assimilation of nitrate by yeasts. *FEMS Microbiol. Rev.* 26 (3), 277–284. <https://doi.org/10.1111/j.1574-6976.2002.tb00615.x>.
- Sudbery, P.E., Gleeson, M.A., Veale, R.A., Ledebor, A.M., Zoetmulder, M.C., 1988. *Hansenula polymorpha* as a novel yeast system for the expression of heterologous genes. *Biochem. Soc. Trans.* 16 (6), 1081–1083. <https://doi.org/10.1042/bst0161081a>.
- Sun, J., Bankston, J.R., Payandeh, J., Hinds, T.R., Zagotta, W.N., Zheng, N., 2014. Crystal structure of the plant dual-affinity nitrate transporter NRT1.1. *Nature* 507 (7490), 73–77. <https://doi.org/10.1038/nature13074>.
- Waadt, R., Schmidt, L.K., Lohse, M., Hashimoto, K., Bock, R., Kudla, J., 2008. Multicolor bimolecular fluorescence complementation reveals simultaneous formation of alternative CBL/CIPK complexes in planta. *Plant J.* 56 (3), 505–516. <https://doi.org/10.1111/j.1365-313X.2008.03612.x>.

- Wallis, J.W., Chrebet, G., Brodsky, G., Rolfe, M., Rothstein, R., 1989. A hyper-recombination mutation in *S. cerevisiae* identifies a novel eukaryotic topoisomerase. *Cell* 58 (2), 409–419. [https://doi.org/10.1016/0092-8674\(89\)90855-6](https://doi.org/10.1016/0092-8674(89)90855-6).
- Wang, W., Hu, B., Li, A., Chu, C., 2020. NRT1.1s in plants: functions beyond nitrate transport. *J. Exp. Bot.* 71 (15), 4373–4379. <https://doi.org/10.1093/jxb/erz554>.
- Wang, X., Feng, C., Tian, L., Hou, C., Tian, W., Hu, B., et al., 2021. A transceptor-channel complex couples nitrate sensing to calcium signaling in *Arabidopsis*. *Mol. Plant* 14 (5), 774–786. <https://doi.org/10.1016/j.molp.2021.02.005>.
- Wang, Y.Y., Cheng, Y.H., Chen, K.E., Tsay, Y.F., 2018. Nitrate transport, signaling, and use efficiency. *Annu. Rev. Plant Biol.* 69, 85–122. <https://doi.org/10.1146/annurev-arplant-042817-040056>.
- Xu, J., Li, H.D., Chen, L.Q., Wang, Y., Liu, L.L., He, L., et al., 2006. A protein kinase, interacting with two calcineurin B-like proteins, regulates K<sup>+</sup> transporter AKT1 in *Arabidopsis*. *Cell* 125 (7), 1347–1360. <https://doi.org/10.1016/j.cell.2006.06.011>.
- Yenush, L., 2016. Potassium and sodium transport in yeast. *Adv. Exp. Med. Biol.* 892, 187–228. [https://doi.org/10.1007/978-3-319-25304-6\\_8](https://doi.org/10.1007/978-3-319-25304-6_8).
- Zheng, Y., Drechsler, N., Rausch, C., Kunze, R., 2016. The *Arabidopsis* nitrate transporter NPF7.3/NRT1.5 is involved in lateral root development under potassium deprivation. *Plant Signal. Behav.* 11 (5), e1176819 <https://doi.org/10.1080/15592324.2016.1176819>.